

# A NEURON-WISE SUBSPACE CORRECTION METHOD FOR THE FINITE NEURON METHOD\*

JONGHO PARK<sup>†</sup>, JINCHAO XU<sup>‡</sup>, AND XIAOFENG XU<sup>§</sup>

**Abstract.** In this paper, we propose a novel algorithm called Neuron-wise Parallel Subspace Correction Method (NPSC) for the finite neuron method that approximates numerical solutions of partial differential equations (PDEs) using neural network functions. Despite extremely extensive research activities in applying neural networks for numerical PDEs, there is still a serious lack of effective training algorithms that can achieve adequate accuracy. Based on recent results on the spectral properties of linear layers and landscape analysis for single neuron problems, we develop a special type of subspace correction method that deals with the linear layer and each neuron in the nonlinear layer separately. An optimal preconditioner that resolves the ill-conditioning of the linear layer is presented, so that the linear layer is trained in a uniform number of iterations with respect to the number of neurons. In each single neuron problem, a good local minimum that prevents dead neurons is found by a superlinearly convergent algorithm. Performance of the proposed method is demonstrated through numerical experiments for function approximation problems and PDEs.

**Key words.** Finite neuron method, Subspace correction method, Training algorithm, Preconditioner, Function approximation, Partial differential equation

**AMS subject classifications.** 65D15, 65N22, 65N30, 65N55, 68T07

**1. Introduction.** Neural networks, thanks to the universal approximation property [8, 25], are promising tools for numerical solutions of partial differential equations (PDEs). Moreover, it was shown in [29] that the approximation properties of neural networks have higher asymptotic approximation rates than that of traditional numerical methods such as the finite element method. Accordingly, there have been extensive research on numerical solutions of PDEs in recent years: physics-informed neural networks [26], the deep Ritz method [10], and the finite neuron method [39], to name a few. Such powerful approximation properties, however, can hardly be observed in numerical experiments even in simple tasks of function approximation. It was shown in [14] that conventional training algorithms such as gradient descent converge too slowly to an accurate solution even for a very simple function. Therefore, applying neural networks to solutions of PDEs must require novel training algorithms, different from the conventional ones for regression, image classification, and pattern recognition tasks. In this viewpoint, there are many works on designing and analyzing training algorithms for neural networks to try to narrow the gap between the theoretical optimum and training results. A hybrid least squares/gradient descent method was proposed in [9]. Plateau phenomena [22] occurring in the gradient dynamics of ReLU shallow neural networks were analyzed in a rigorous manner in [1], and a training algorithm called active neuron least squares was designed to avoid

---

\*Submitted to arXiv January 8th, 2023.

**Funding:** This work was supported in part by the NRF grant funded by MSIT (No. 2021R1C1C2095193), and in part by the KAUST Baseline Research Fund.

<sup>†</sup>Natural Science Research Institute, KAIST, Daejeon 34141, Korea ([jongho.park@kaist.ac.kr](mailto:jongho.park@kaist.ac.kr), <https://sites.google.com/view/jonghopark>).

<sup>‡</sup>Computer, Electrical and Mathematical Science and Engineering Division, King Abdullah University of Science and Technology (KAUST), Thuwal 23955, Saudi Arabia ([jinchao.xu@kaust.edu.sa](mailto:jinchao.xu@kaust.edu.sa)). Department of Mathematics, Pennsylvania State University, University Park, PA 16802, USA ([xu@math.psu.edu](mailto:xu@math.psu.edu)).

<sup>§</sup>Computer, Electrical and Mathematical Science and Engineering Division, King Abdullah University of Science and Technology (KAUST), Thuwal 23955, Saudi Arabia ([xiaofeng.xu@kaust.edu.sa](mailto:xiaofeng.xu@kaust.edu.sa)).

plateau phenomena in [2]. As a completely different approach, the orthogonal greedy algorithm was shown to achieve an optimal convergence rate [31] with respect to the number of neurons when it is applied to certain shallow neural networks in [30].

A surprising recent result on training of neural networks shows that optimizing the linear layer parameters in a neural network is one bottleneck that leads to a large number of iterations of a gradient-based method. More precisely, it was proven in [14] that optimizing the linear layer parameters in a ReLU shallow neural network requires solving a very ill-conditioned linear problem in general. This work motivates us to separately design efficient solvers for the outer linear layer and the inner nonlinear layer, respectively, and train them alternately.

Meanwhile, there have been some encouraging works on learning a single neuron, a more simplified model than a nonlinear layer. Convergence analyses of gradient methods for the single neuron problem with ReLU activation were presented in [32, 34, 42] under various assumptions on input distributions. The case of a single ReLU neuron with bias was analyzed in [36]. All of these results show that the global convergence of gradient methods for the single ReLU neuron problem can be attained under certain conditions. Hence, learning a single neuron can be regarded as a much more hopeful task than learning a nonlinear layer with multiple neurons.

In this paper, we use the idea of subspace correction [38], which is well-known in the fields of numerical analysis and scientific computing. Subspace correction methods provide a unified framework to design and analyze many modern iterative numerical methods such as block coordinate descent, multigrid, and domain decomposition methods. In subspace correction methods, the solution space of a target problem is decomposed into a sum of subspaces, and local problems defined on subspaces are solved separately in either sequential or parallel manner. Then a solution of the whole problem is constructed by assembling the solutions of the local problems appropriately. Mathematical theory of subspace correction methods for convex optimization problems can be found in [23, 33]. Subspace correction methods have been successfully applied to various nonlinear optimization problems appearing in engineering fields (see, e.g., [3, 18]). In particular, there have been successful applications of block coordinate descent methods [37] for training of neural networks [43, 44]. Therefore, we expect that the idea of the subspace correction method is also suitable for training of neural networks.

Inspired by the above works, we propose a new training algorithm called Neuron-wise Parallel Subspace Correction Method (NPSC), which is a special type of subspace correction method for the finite neuron method [39]. The proposed method utilizes a space decomposition for the linear layer and each individual neuron. In the first step of each epoch of the NPSC, the linear layer is fully trained by solving a relevant linear system. This resolves ill-conditioning of the linear layer. We design an optimal preconditioner for the linear layer problem in one-dimension, based on the relation between ReLU neural networks and linear finite elements investigated in [11, 14]. In the second step, we train each single neuron in parallel, taking advantages of better convergence properties of learning a single neuron explained above. Each neuron is trained by a superlinearly convergent algorithm [20]. Finally, an update for the parameters in the nonlinear layer is computed by assembling the corrections obtained in the local problems for each neuron. Due to the intrinsic parallel structure, NPSC is suitable for parallel computation on distributed memory computers. We present applications of NPSC to various function approximation problems and PDEs, and numerically verify that it outperforms conventional training algorithms.

The rest of this paper is organized as follows. In [section 2](#), we summarize key

features of the finite neuron method with ReLU shallow neural networks. An optimal preconditioner for the linear layer in one-dimension is presented in [section 3](#). NPSC, our proposed algorithm, is presented in [section 4](#). Applications of NPSC to various function approximation problems and PDEs are presented in [section 5](#) to demonstrate the effectiveness of NPSC. We conclude the paper with remarks in [section 6](#).

**2. Finite neuron method.** In this section, we introduce the finite neuron method [\[39\]](#) with ReLU shallow neural networks, which numerically solves elliptic PDEs using solution spaces based on neural networks. Then we provide a brief explanation of why finding an accurate solution of the finite neuron method using conventional training algorithms such as gradient descent is difficult by illustrating the ill-conditioning of ReLU neural networks [\[14\]](#).

Let  $\Omega \subset \mathbb{R}^d$  be a bounded domain and let  $f \in L^2(\Omega)$ . We consider the following model problem:

$$(2.1) \quad \min_{u \in V} \left\{ \frac{1}{2} a(u, u) - \int_{\Omega} f u \, dx \right\},$$

where  $a(\cdot, \cdot)$  is a continuous, coercive, and symmetric bilinear form defined on a Hilbert space  $V \subset L^2(\Omega)$ . It is well-known that various elliptic boundary value problems can be formulated as optimization problems of the form [\(2.1\)](#) [\[39\]](#).

A ReLU shallow neural network with  $n$  neurons and a  $d$ -dimensional input  $x \in \mathbb{R}^d$  is given by

$$(2.2) \quad u(x; \theta) = \sum_{i=1}^n a_i \sigma(\omega_i \cdot x + b_i), \quad \theta = \{a, \omega, b\} = \{(a_i)_{i=1}^n, (\omega_i)_{i=1}^n, (b_i)_{i=1}^n\},$$

where  $\theta$  is the collection of parameters consisting of  $a_i \in \mathbb{R}$ ,  $\omega_i \in \mathbb{R}^d$ , and  $b_i \in \mathbb{R}$  for  $1 \leq i \leq n$ , and  $\sigma: \mathbb{R} \rightarrow \mathbb{R}$  is the ReLU activation function defined by  $\sigma(x) = \max\{0, x\}$ . The neural network [\(2.2\)](#) possesses total  $(d+2)n$  parameters. The collection of all neural network functions of the form [\(2.2\)](#) is denoted by  $\Sigma_n$ , i.e.,

$$\Sigma_n = \left\{ v(x) = \sum_{i=1}^n a_i \sigma(\omega_i \cdot x + b_i) : a_i \in \mathbb{R}, \omega_i \in \mathbb{R}^d, b_i \in \mathbb{R} \right\}.$$

The space  $\Sigma_n$  enjoys the universal approximation property [\[8, 25\]](#), namely, any function with sufficient regularity can be uniformly approximated by functions in  $\Sigma_n$ . Recent results on the approximation property of  $\Sigma_n$  can be found in [\[29, 31\]](#).

In the finite neuron method, we consider the Galerkin approximation of [\(2.1\)](#) on the space  $\Sigma_n$ :

$$\min_{u \in \Sigma_n} \left\{ \frac{1}{2} a(u, u) - \int_{\Omega} f u \, dx \right\},$$

which is equivalent to

$$(2.3) \quad \min_{\theta \in \Theta} \left\{ E(\theta) := \frac{1}{2} a(u(x; \theta), u(x; \theta)) - \int_{\Omega} f(x) u(x; \theta) \, dx \right\},$$

where  $\Theta = \mathbb{R}^{(d+2)n}$  is the parameter space. Thanks to the superior approximation property of  $\Sigma_n$  [\[29\]](#), it is expected the finite neuron method yields a more accurate numerical solution than that of traditional numerical methods. In particular, it was observed in [\[11\]](#) that [\(2.3\)](#) provides a better approximation result than conventional adaptive finite element methods in one dimension.

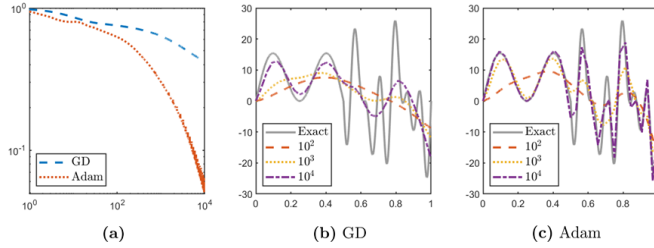


FIG. 1. Numerical results for the function approximation problem (2.5). (a) Decay of the relative energy error  $\frac{E_M(a^{(k)}) - E_M(M^{-1}\beta)}{|E_M(M^{-1}\beta)|}$  in the gradient descent method (GD) and Adam, where  $k$  denotes the number of iterations. (b, c) Exact solution and its approximations generated by various numbers of iterations of GD and Adam ( $n = 2^5$ ).

**2.1. Ill-conditioning of the linear layer.** From the structure of the neural network (2.2), we say that the parameter  $a$  belongs to the linear layer and  $\omega$  and  $b$  belong to the nonlinear layer. In general, optimizing the parameters in the linear layer is a less challenging task thanks to many available linear solvers. However, we explain that even optimizing parameters in the linear layer becomes a bottleneck if we use simple gradient-based methods. A very large number of iterations is needed to achieve satisfactory accuracy.

To illustrate the ill-conditioning, we consider  $\Omega = (0, 1) \subset \mathbb{R}$  and the following bilinear form

$$(2.4) \quad a(u, v) = \int_{\Omega} uv \, dx, \quad u, v \in V, \quad V = L^2(\Omega)$$

in (2.3). We obtain the  $L^2$ -function approximation problem, which is the most elementary instance of (2.3). We fix the parameters  $\omega$  and  $b$  in (2.3) as follows:

$$\omega_i = 1, \quad b_i = -\frac{i-1}{n}, \quad 1 \leq i \leq n.$$

Then (2.3) is written as

$$(2.5) \quad \min_{a \in \mathbb{R}^n} \left\{ E_M(a) := \frac{1}{2} a^T M a - \beta^T a \right\},$$

where  $M \in \mathbb{R}^{n \times n}$  and  $\beta \in \mathbb{R}^n$  are given by

$$M_{ij} = \int_{\Omega} \sigma \left( x - \frac{j-1}{n} \right) \sigma \left( x - \frac{i-1}{n} \right) dx, \quad 1 \leq i, j \leq n.$$

$$\beta_i = \int_{\Omega} f(x) \sigma \left( x - \frac{i-1}{n} \right) dx,$$

When we solve the minimization problem (2.5) by a gradient-based method such as the gradient descent method or Adam [15], the convergence rate depends on the condition number  $\kappa(M)$  of  $M$ . It was recently proved in [14, Theorem 1] that  $M$  is very ill-conditioned. This result is stated in the following proposition.

PROPOSITION 2.1. In (2.5), the condition number  $\kappa(M)$  of the matrix  $M$  satisfies

$$\kappa(M) = O(n^4).$$

The condition number  $\kappa(M)$  becomes exceedingly large when  $n$  increases, so that the convergence of simple gradient-based methods thus becomes extremely slow. We now demonstrate the poor convergence of the gradient descent method and Adam for solving (2.5) with  $f$  given by

$$(2.6) \quad f(x) = \begin{cases} 10(\sin 2\pi x + \sin 6\pi x), & \text{if } 0 < x < \frac{1}{2}, \\ 10(\sin 8\pi x + \sin 18\pi x + \sin 26\pi x), & \text{if } \frac{1}{2} \leq x < 1. \end{cases}$$

In both methods, the learning rate  $\tau$  is chosen as  $\tau = 2/(\lambda_{\min}(M) + \lambda_{\max}(M))$ , which is optimal in the sense of [35, Lemma C.5];  $\lambda_{\min}$  and  $\lambda_{\max}$  stand for the minimum and maximum eigenvalues, respectively. We use the zero initial guess. One can observe in Figure 1(a) that the convergence rates of both methods are fairly slow even if  $n$  is not so large; the relative energy error  $\frac{E_M(a^{(k)}) - E_M(M^{-1}\beta)}{|E_M(M^{-1}\beta)|}$  does not reach  $10^{-2}$  with  $10^4$  iterations, where  $k$  denotes the number of iterations. Moreover, as shown in Figure 1(b, c), both methods provide poor numerical approximations to  $f$  despite of large numbers of iterations. These results clearly verify the difficulty of optimizing the parameter  $a$  in (2.2) by conventional training algorithms.

**3. Optimal preconditioner for the linear layer.** In this section, we propose an optimal preconditioner for the linear layer in one dimension. Using the proposed preconditioner, the linear layer can be fully trained within a uniform number of iterations with respect to the number of neurons  $n$ .

For simplicity, we set  $\Omega = (0, 1) \subset \mathbb{R}$  in (2.3). Fixing the parameters  $\omega$  and  $b$  in the nonlinear layer, (2.3) reduces to the following minimization problem with respect to  $a$ :

$$(3.1) \quad \min_{a \in \mathbb{R}^n} \left\{ \frac{1}{2} a^T K a - \beta^T a \right\},$$

where  $K \in \mathbb{R}^{n \times n}$  and  $\beta \in \mathbb{R}^n$  are given by

$$(3.2) \quad \begin{aligned} K_{ij} &= a(\sigma(\omega_j x + b_j), \sigma(\omega_i x + b_i)), \\ \beta_i &= \int_{\Omega} f(x) \sigma(\omega_i x + b_i) dx, \end{aligned} \quad 1 \leq i, j \leq n.$$

Let

$$x_i = -\frac{b_i}{\omega_i}, \quad 1 \leq i \leq n,$$

be the nodal point determined by the ReLU function  $\psi_i(x) = \sigma(\omega_i x + b_i)$ . We denote the number of the nodal points inside  $\Omega$  by  $n_{\Omega}$ . Without loss of generality, we assume the following:

$$(3.3a) \quad \psi_i \not\equiv 0 \text{ on } \Omega, \quad 1 \leq i \leq n,$$

$$(3.3b) \quad n_{\Omega} \geq n - 2,$$

$$(3.3c) \quad x_1, \dots, x_{n_{\Omega}} \in \Omega \text{ and } x_1 < \dots < x_{n_{\Omega}},$$

$$(3.3d) \quad x_{n_{\Omega}+1}, \dots, x_n \in \mathbb{R} \setminus \Omega \text{ and } x_{n_{\Omega}+1} < \dots < x_n.$$

The assumption (3.3a) requires that no  $\psi_i$  vanishes on  $\Omega$  because otherwise they do not contribute to the minimization problem (3.1). The assumption (3.3b) requires at most

two neurons with nodal points outside  $\Omega$ . This is because the corresponding ReLU functions become linearly dependent on  $\Omega$  if there are more than two neurons with nodal points outside  $\Omega$ . Finally, the assumptions (3.3c) and (3.3d) can be satisfied under an appropriate reordering.

Under (3.3), it is proved in [11, Theorem 2.1] that  $\{\psi_i\}_{i=1}^n$  are linearly independent on  $\Omega$ . It is easy to see  $K$  is symmetric and positive definite (SPD). Let  $\mathcal{A}: V \rightarrow V$  be a bijective linear operator such that

$$(3.4) \quad a(u, v) = \int_{\Omega} (\mathcal{A}u)v \, dx, \quad u, v \in V.$$

Writing  $\Psi = [\psi_1, \dots, \psi_n]^T$ , we have

$$K = \int_{\Omega} (\mathcal{A}\Psi(x))\Psi(x)^T \, dx,$$

where  $\mathcal{A}$  is applied entrywise.

Before we present the optimal preconditioner, we state the following lemma that is useful for the construction of the proposed preconditioner.

LEMMA 3.1. *For two positive integers  $m \geq n$ , let  $A, B \in \mathbb{R}^{m \times m}$  be two SPD matrices and let  $R \in \mathbb{R}^{n \times m}$  be a surjective matrix. Then  $RB^{-1}R^T$  is SPD and*

$$\kappa\left((RB^{-1}R^T)^{-1}RAR^T\right) \leq \kappa(BA).$$

*Proof.* It is easy to see that  $B^{-1}$  is SPD and  $R^T$  is injective. Then we have

$$\langle RB^{-1}R^T\alpha, \alpha \rangle = \langle B^{-1}R^T\alpha, R^T\alpha \rangle > 0, \quad \forall \alpha \neq \mathbf{0}.$$

Hence,  $RB^{-1}R^T$  is also SPD.

One can establish a lower bound for the minimum eigenvalue of the matrix  $(RB^{-1}R^T)^{-1}RAR^T$  as follows:

$$(3.5) \quad \lambda_{\min}\left((RB^{-1}R^T)^{-1}RAR^T\right) = \min_{\alpha \neq \mathbf{0}} \frac{\alpha^T RAR^T \alpha}{\alpha^T RB^{-1}R^T \alpha} \\ = \min_{\substack{\bar{\alpha} \in \text{ran } R^T \\ \bar{\alpha} \neq \mathbf{0}}} \frac{\bar{\alpha}^T A \bar{\alpha}}{\bar{\alpha}^T B^{-1} \bar{\alpha}} \geq \min_{\bar{\alpha} \neq \mathbf{0}} \frac{\bar{\alpha}^T A \bar{\alpha}}{\bar{\alpha}^T B^{-1} \bar{\alpha}} = \lambda_{\min}(BA).$$

In the same manner, we have

$$(3.6) \quad \lambda_{\max}\left((RB^{-1}R^T)^{-1}RAR^T\right) \leq \lambda_{\max}(BA).$$

Combining (3.5) and (3.6) yields the desired result.  $\square$

Now we are ready to construct our proposed preconditioner, which resolves the issue of ill-conditioning explained in section 2. We define

$$\psi_L(x) = x, \quad \psi_R(x) = 1 - x,$$

and write  $\bar{\Psi} = [\psi_1, \dots, \psi_{n_{\Omega}}, \psi_L, \psi_R]^T$ . Since each  $\psi_i$ ,  $n_{\Omega} + 1 \leq i \leq n$ , is linear on  $\Omega$ , we have

$$\psi_i = \psi_i(1)\psi_L + \psi_i(0)\psi_R \quad \text{on } \Omega.$$

Hence, we readily get  $\Psi = R\bar{\Psi}$  on  $\Omega$ , where

$$(3.7) \quad R = \begin{bmatrix} I_{n_\Omega} & \mathbf{0} \\ \mathbf{0} & \tilde{R} \end{bmatrix} \in \mathbb{R}^{n \times (n_\Omega+2)}, \quad \tilde{R} = \begin{bmatrix} \psi_{n_\Omega+1}(1) & \psi_{n_\Omega+1}(0) \\ \vdots & \vdots \\ \psi_n(1) & \psi_n(0) \end{bmatrix} \in \mathbb{R}^{(n-n_\Omega) \times 2}.$$

In (3.7),  $I_{n_\Omega}$  denotes the  $\mathbb{R}^{n_\Omega \times n_\Omega}$  identity matrix.

We define

$$(3.8) \quad \bar{K} = \int_{\Omega} (\mathcal{A}\bar{\Psi}(x))\bar{\Psi}(x)^T dx.$$

It is easy to see  $M = R\bar{K}R^T$ . Invoking [11, Theorem 2.1] implies that the entries of  $\bar{\Psi}$  are linearly independent, so that they form a basis for the space  $V_{n_\Omega+2}$  of continuous and piecewise linear functions on the grid  $0 < x_1 < \dots < x_{n_\Omega} < 1$ .

If we set  $\bar{\Psi}^+ = [\psi_1^+, \dots, \psi_{n_\Omega}^+, \psi_L, \psi_R]^T$ , where

$$\psi_i^+(x) = \sigma(x - x_i), \quad 1 \leq i \leq n_\Omega,$$

then by direct calculation we get

$$(3.9) \quad \psi_i = \begin{cases} \omega_i \psi_i^+, & \text{if } \omega_i \geq 0, \\ \omega_i(1 - x_i)\psi_L - \omega_i \psi_i^+ - \omega_i x_i \psi_R, & \text{otherwise.} \end{cases}$$

Using (3.9), it is straightforward to construct a matrix  $B_1 \in \mathbb{R}^{(n_\Omega+2) \times (n_\Omega+2)}$  satisfying

$$(3.10) \quad \bar{\Psi} = B_1 \bar{\Psi}^+.$$

The matrix  $B_1$  is nonsingular since both the entries of  $\bar{\Psi}$  and those of  $\bar{\Psi}^+$  form bases for the space  $V_{n_\Omega+2}$  [11].

Meanwhile,  $V_{n_\Omega+2}$  admits the standard hat basis  $\{\phi_1, \dots, \phi_{n_\Omega}, \phi_L, \phi_R\}$ , which is given by

$$\phi_i(x) = \begin{cases} \frac{x - x_{i-1}}{x_i - x_{i-1}}, & \text{if } x \in (x_{i-1}, x_i], \\ \frac{x - x_{i+1}}{x_i - x_{i+1}}, & \text{if } x \in [x_i, x_{i+1}), \\ 0, & \text{otherwise,} \end{cases} \quad 1 \leq i \leq n_\Omega,$$

$$\phi_L(x) = \begin{cases} -\frac{x - x_1}{x_1}, & \text{if } x \in (0, x_1], \\ 0, & \text{otherwise,} \end{cases} \quad \phi_R(x) = \begin{cases} \frac{x - x_{n_\Omega}}{1 - x_{n_\Omega}}, & \text{if } x \in [x_{n_\Omega}, 1), \\ 0, & \text{otherwise,} \end{cases}$$

with abuse of notation  $x_{-1} = 0$  and  $x_{n_\Omega+1} = 1$ . Similar to (3.8), we write  $\bar{\Phi} = [\phi_1, \dots, \phi_{n_\Omega}, \phi_L, \phi_R]^T$  and set

$$\bar{K}_\phi = \int_{\Omega} (\mathcal{A}\bar{\Phi}(x))\bar{\Phi}(x)^T dx.$$

One can verify the following relation between the entries of  $\bar{\Phi}$  and those of  $\bar{\Psi}^+$  by

direct calculation:

(3.11)

$$\begin{aligned}\phi_1 &= \frac{1}{x_1}\psi_L - \frac{x_2}{(x_2-x_1)x_1}\psi_1^+ + \frac{1}{x_2-x_1}\psi_2^+, \\ \phi_i &= \frac{1}{x_i-x_{i-1}}\psi_{i-1}^+ - \frac{x_{i+1}-x_{i-1}}{(x_{i+1}-x_i)(x_i-x_{i-1})}\psi_i^+ + \frac{1}{x_{i+1}-x_i}\psi_{i+1}^+, \quad 2 \leq i \leq n_\Omega - 1, \\ \phi_{n_\Omega} &= \frac{1}{x_{n_\Omega}-x_{n_\Omega-1}}\psi_{n_\Omega-1}^+ - \frac{1-x_{n_\Omega-1}}{(1-x_{n_\Omega})(x_{n_\Omega}-x_{n_\Omega-1})}\psi_{n_\Omega}^+, \\ \phi_L &= -\frac{1-x_1}{x_1}\psi_L + \frac{1}{x_1}\psi_1^+ + \psi_R, \\ \phi_R &= \frac{1}{1-x_n}\psi_{n_\Omega}^+.\end{aligned}$$

Hence, we can construct a matrix  $B_2 \in \mathbb{R}^{(n_\Omega+2) \times (n_\Omega+2)}$  such that

$$(3.12) \quad \bar{\Phi} = B_2 \bar{\Psi}^+$$

explicitly using (3.11). Combining (3.10) and (3.12) yields

$$(3.13) \quad \bar{\Phi} = B \bar{\Psi},$$

where  $B = B_2 B_1^{-1}$ . Equation (3.13) implies that two matrices  $\bar{K}$  and  $\bar{K}_\phi$  are related as follows:

$$(3.14) \quad \bar{K} = \int_{\Omega} (\mathcal{A} \bar{\Psi}(x)) \bar{\Psi}(x)^T dx = \int_{\Omega} B^{-1} (\mathcal{A} \bar{\Phi}(x)) \bar{\Phi}(x)^T B^{-T} dx = B^{-1} \bar{K}_\phi B^{-T}.$$

Since  $M = R \bar{K} R^T$ , invoking Lemma 3.1, setting  $\bar{P} = B^T \bar{K}_\phi^{-1} B$  and

$$(3.15) \quad P = \left( R \bar{P}^{-1} R^T \right)^{-1}$$

completes the construction of the proposed preconditioner, where  $R$  was defined in (3.7). We summarize our main result described above in the following theorem.

**THEOREM 3.2.** *Let  $\Omega = (0, 1) \subset \mathbb{R}$  and let  $K \in \mathbb{R}^{n \times n}$  be the matrix defined in (3.2). Assume that (3.3) holds. Then the preconditioner  $P \in \mathbb{R}^{n \times n}$  given in (3.15) satisfies*

$$\kappa(PK) = O(1),$$

*i.e.,  $\kappa(PK)$  has an upper bound independent of  $n$ ,  $\omega$ , and  $b$ .*

In spite of somewhat complicated structure of the proposed preconditioner  $P$ , it can be implemented very efficiently, requiring only  $O(n)$  elementary arithmetic operations. Details of the implementation of the proposed preconditioner are discussed in Appendix A.

*Remark 3.3.* In the case of the  $L^2$ -function approximation problem (2.4), we can construct an alternative preconditioner  $P_{\text{diag}}$  whose computational cost is a bit cheaper than  $P$ . Let  $\bar{P}_{\text{diag}} = B^T \text{diag}(\bar{K}_\phi)^{-1} B$ . It follows from (3.14) that

$$\bar{P}_{\text{diag}} \bar{K} = B^T \text{diag}(\bar{K}_\phi)^{-1} B \bar{K} = B^T \text{diag}(\bar{K}_\phi)^{-1} \bar{K}_\phi B^{-T}.$$



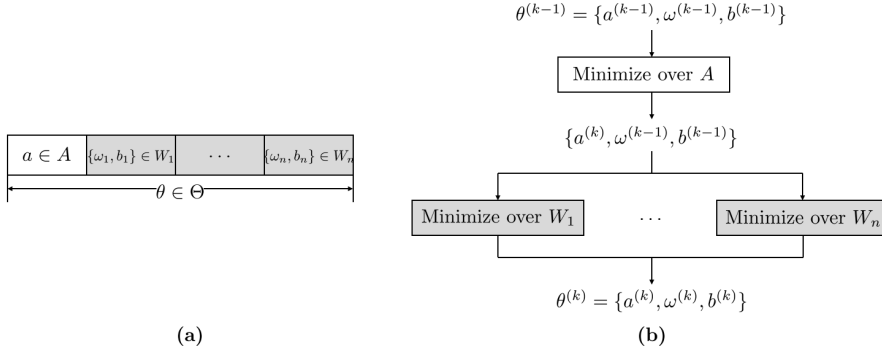


FIG. 2. (a) Space decomposition of the solution space  $\Theta$  of (2.3) into subspaces  $A$  and  $\{W_i\}_{i=1}^n$ . (b) Subspace correction procedure of NPSC.

In (2.4),  $\bar{K}_\phi$  is a mass matrix for the linear finite element method defined on the grid  $0 < x_1 < \dots < x_{n_\Omega} < 1$ , so that it satisfies  $\kappa(\text{diag}(\bar{K}_\phi)^{-1}\bar{K}_\phi) = O(1)$ . Then we have

$$\kappa(\bar{P}_{\text{diag}}\bar{K}) = \kappa(B^T \text{diag}(\bar{K}_\phi)^{-1}\bar{K}_\phi B^{-T}) = \kappa(\text{diag}(\bar{K}_\phi)^{-1}\bar{K}_\phi) = O(1).$$

Therefore,  $P_{\text{diag}} = (R\bar{P}_{\text{diag}}^{-1}R^T)^{-1}$  satisfies  $\kappa(P_{\text{diag}}K) = O(1)$  by Lemma 3.1. It is evident that the computational cost of  $\text{diag}(\bar{K}_\phi)^{-1}$  is cheaper than that of  $\bar{K}_\phi^{-1}$ .

**4. Neuron-wise Parallel Subspace Correction Method (NPSC).** In this section, we introduce NPSC, a subspace correction method [38] that deals with the linear layer and each neuron in the nonlinear layer separately for solving (2.3). Thanks to the preconditioner proposed in the previous section, the linear layer of the neural network (2.2) can be fully trained with a cheap computational cost. This is the main motivation for separating the training of the linear and nonlinear layers.

We first present a space decomposition for NPSC. The parameter space  $\Theta$  admits a natural decomposition  $\Theta = A \oplus W$ , where  $A = \mathbb{R}^n$  and  $W = \mathbb{R}^{(d+1)n}$  are the spaces for  $a$  and  $\{\omega, b\}$ , respectively, and  $\oplus$  denotes direct sum. Since any  $\{\omega, b\} \in W$  consists of the parameters  $(\{\omega_i, b_i\})_{i=1}^n$  from  $n$  neurons,  $W$  can be further decomposed as  $W = \bigoplus_{i=1}^n W_i$ , where  $W_i = \mathbb{R}^{d+1}$  is the space for  $\{\omega_i, b_i\}$ . Finally, we have the following space decomposition of  $\Theta$ :

$$(4.1) \quad \Theta = A \oplus \bigoplus_{i=1}^n W_i.$$

A graphical description for the space decomposition (4.1) is presented in Figure 2(a).

NPSC, our proposed method, is presented in Algorithm 4.1. It is a subspace correction method [38] for (2.3) based on the space decomposition (4.1). At the  $k$ th epoch, NPSC updates the parameter  $a$  first by minimizing the loss function with respect to  $a$ , then it updates the parameters in each neuron by minimizing  $E$  with respect to  $\{\omega_i, b_i\}$  in parallel. The update of  $\{\omega_i, b_i\}$  is relaxed by an appropriate learning rate  $\tau_k > 0$  as in the existing parallel subspace correction methods for optimization problems [18, 33]. The overall structure of NPSC is depicted in Figure 2(b). In the remainder of this section, we discuss different parts of Algorithm 4.1 in detail.

**4.1. Adjustment of parameters.** Here, we discuss the necessity of adjusting parameters during the training. We call that a neuron with parameter  $\{\omega_i, b_i\}$  is dead

**Algorithm 4.1** Neuron-wise Parallel Subspace Correction Method (NPSC) for (2.3)

Choose an initial guess  $\theta^{(0)} = \{a^{(0)}, \omega^{(0)}, b^{(0)}\}$  and an initial learning rate  $\tau_0 = 1$ .

**for**  $k = 0, \dots, T - 1$  **do**

Adjust  $\{\omega^{(k)}, b^{(k)}\}$  to avoid linear dependence of the neurons (see Algorithm 4.2).

$a^{(k+1)} \in \arg \min_{a \in A} E(\{a, \omega^{(k)}, b^{(k)}\})$  (see (4.3))

**for**  $i = 1, \dots, n$  **in parallel do**

(4.2)

$$\{\omega_i^{(k+\frac{1}{2})}, b_i^{(k+\frac{1}{2})}\} \in \arg \min_{\{\omega_i, b_i\} \in W_i} E \left( \left\{ a^{(k+1)}, \omega_i \oplus \bigoplus_{j \neq i} \omega_j^{(k)}, b_i \oplus \bigoplus_{j \neq i} b_j^{(k)} \right\} \right)$$

**end for**

Determine the learning rate  $\tau_k$  by backtracking (see Algorithm 4.3).

**for**  $i = 1, \dots, n$  **in parallel do**

$$\omega_i^{(k+1)} = (1 - \tau_k) \omega_i^{(k)} + \tau_k \omega_i^{(k+\frac{1}{2})}$$

$$b_i^{(k+1)} = (1 - \tau_k) b_i^{(k)} + \tau_k b_i^{(k+\frac{1}{2})}$$

**end for**

**end for**

if  $\sigma(\omega_i \cdot x + b_i)$  vanishes on the domain  $\Omega$ . In [36, Theorem 3.1], it was shown that a neuron is initialized as dead with probability close to half if we employ a usual random initialization scheme [12]. A similar observation was made in [19]. Such a dead neuron makes the functions  $\{\sigma(\omega_i \cdot x + b_i)\}_{i=1}^n$  linearly dependent. Meanwhile, linear dependence may occur by neurons whose nodal points are outside  $\Omega$ ; such scenarios are summarized in Proposition 4.1.

PROPOSITION 4.1. *In the neural network (2.2), we have the following:*

1. *If a neuron satisfies  $b_i \leq -\max_{x \in \bar{\Omega}} \omega_i \cdot x$ , then it is dead.*
2. *If there are more than  $d + 1$  neurons such that  $b_i \geq -\min_{x \in \bar{\Omega}} \omega_i \cdot x$ , then the functions  $\sigma(\omega_i \cdot x + b_i)$  corresponding to these neurons are linearly dependent on  $\Omega$ .*

*Proof.* If  $b_i \leq -\max_{x \in \bar{\Omega}} \omega_i \cdot x$  for some  $i$ , then we have

$$\omega_i \cdot x + b_i \leq \max_{x \in \bar{\Omega}} \omega_i \cdot x + b_i \leq 0 \quad \text{in } \Omega.$$

Hence,  $\sigma(\omega_i \cdot x + b_i) = 0$  on  $\Omega$ , which means that the corresponding neuron is dead.

Now, we suppose that  $b_i \geq -\min_{x \in \bar{\Omega}} \omega_i \cdot x$  for  $1 \leq i \leq d + 2$ . Then we have

$$\omega_i \cdot x + b_i \geq \min_{x \in \bar{\Omega}} \omega_i \cdot x + b_i \geq 0 \quad \text{in } \Omega.$$

This implies that  $\sigma(\omega_i \cdot x + b_i) = \omega_i \cdot x + b_i$  on  $\Omega$ , i.e., each  $\sigma(\omega_i \cdot x + b_i)$  is linear on  $\Omega$ . Since the dimension of the space of all linear functions on  $\Omega$  is  $d + 1$ ,  $\{\sigma(\omega_i \cdot x + b_i)\}_{i=1}^{d+2}$  are linearly dependent on  $\Omega$ .  $\square$

Linear dependence of the functions  $\{\sigma(\omega_i \cdot x + b_i)\}_{i=1}^n$  in the neural network (2.2) should be avoided because it means that several neurons are redundant and they are

not utilized to improve the approximability of (2.2). Proposition 4.1 motivates us to consider an adjustment procedure for  $\{\omega^{(k)}, b^{(k)}\}$  when we enter the  $k$ th iteration of NPSC so that linear dependence does not occur. Algorithm 4.2 summarizes the adjustment procedure for a given  $\{\omega, b\} \in W$ .

---

**Algorithm 4.2** Adjustment for  $\{\omega, b\}$  in Algorithm 4.1
 

---

```

Set  $m = 0$ .
for  $i = 1, \dots, n$  do
  Set  $\omega_i \leftarrow \frac{\omega_i}{|\omega_i|}$  and  $b_i \leftarrow \frac{b_i}{|\omega_i|}$ .
  if  $b_i \leq -\max_{x \in \bar{\Omega}} \omega_i \cdot x$  then
    Reset  $b_i \in \mathbb{R}$  such that  $b_i \sim \text{Uniform} \left( -\max_{x \in \bar{\Omega}} \omega_i \cdot x, -\min_{x \in \bar{\Omega}} \omega_i \cdot x \right)$ .
  end if
  if  $b_i \geq -\min_{x \in \bar{\Omega}} \omega_i \cdot x$  then
    if  $m > d + 1$  then
      Reset  $b_i \in \mathbb{R}$  such that  $b_i \sim \text{Uniform} \left( -\max_{x \in \bar{\Omega}} \omega_i \cdot x, -\min_{x \in \bar{\Omega}} \omega_i \cdot x \right)$ .
    else
       $m \leftarrow m + 1$ 
    end if
  end if
end for

```

---

Since  $\omega_i$  determines the direction of a function  $\sigma(\omega_i \cdot x + b_i)$ , we may normalize  $\{\omega_i, b_i\}$  so that  $|\omega_i| = 1$  in Algorithm 4.2. Then, for each  $b_i$  that is not on the interval between the minimum and maximum of  $\omega_i \cdot x$ , we relocate it on the interval. This relocation step helps avoid the scenario of linear dependence in neurons described in Proposition 4.1.

In Algorithm 4.2, evaluations of the extrema of  $\omega_i \cdot x$  on  $\bar{\Omega}$  are simple linear programs, so that they can be done efficiently by conventional algorithms for linear programming [21]. In particular, if  $\Omega$  is a polyhedral domain, we can simply compute  $\omega_i \cdot x$  at all the vertices of  $\Omega$  and take the extrema among them.

**4.2.  $a$ -minimization problem.** As we discussed in section 3, the  $a$ -minimization problem in Algorithm 4.1 can be represented as a quadratic optimization problem of the form (3.1). Equivalently, it suffices to solve a system of linear equations

$$(4.3) \quad Ka = \beta,$$

where  $K$  and  $\beta$  are defined in a similar manner as (3.2). Since it is guaranteed by Algorithm 4.2 that  $K$  is SPD, (4.3) can be solved by the preconditioned conjugate gradient method (see, e.g., [27]). Equipped with the preconditioner proposed in section 3, the preconditioned conjugate gradient method always finds a solution of (4.3) up to a certain level of precision within a uniform number of iterations with respect to  $n$ ,  $\omega^{(k)}$ , and  $b^{(k)}$ .

**4.3.  $\{\omega_i, b_i\}$ -minimization problems.** Training the nonlinear layer is challenging because of its nonconvexity. Moreover, it was shown in [19] that training of ReLU networks usually suffers from dead neurons. In the following, we discuss that training

each neuron in the nonlinear layer separately has an advantage that some “good” local minima that avoid dead neurons can be found.

We consider the  $\{\omega_i, b_i\}$ -minimization problem (4.2) in Algorithm 4.1 for a fixed  $i$ . We may assume that  $a_i \neq 0$ ; otherwise, the minimization problem becomes trivial. Under some elementary manipulations, (4.2) is rewritten as

$$(4.4) \quad \min_{\{\omega_i, b_i\} \in \mathbb{R}^{d+1}} \left\{ E_i(\omega_i, b_i) := \frac{1}{2} a (\psi_i, \psi_i) - \int_{\Omega} F \psi_i dx \right\},$$

where  $\psi_i(x) = \sigma(\omega_i \cdot x + b_i)$  and  $F \in L^2(\Omega)$  is a function determined in terms of  $f$ ,  $a^{(k+1)}$ ,  $\omega_j^{(k)}$ , and  $b_j^{(k)}$  for  $j \neq i$ . We first present an existing result [36, Theorem 4.2] on single neuron training (4.4) under a particular assumption.

PROPOSITION 4.2. *In the single neuron problem (4.4), we assume that*

$$(4.5) \quad F(x) = \sigma(\hat{\omega}_i \cdot x + \hat{b}_i)$$

for some  $\hat{\omega}_i \in \mathbb{R}^d$  and  $\hat{b}_i \in \mathbb{R}$ . Then any critical point  $\{\omega_i^*, b_i^*\} \in \mathbb{R}^{d+1}$  such that  $\sigma(\omega_i^* \cdot x + b_i^*) \not\equiv 0$  on  $\Omega$  is a global minimum.

Proposition 4.2 implies that, under the assumption (4.5) on  $F$ , if we choose an initial guess  $\{\omega_i^{(0)}, b_i^{(0)}\}$  such that  $E_i(\omega_i^{(0)}, b_i^{(0)}) < E_i(\mathbf{0}, 0)$  for a monotone training algorithm, then the algorithm converges to a global minimum. Note that the condition  $E_i(\omega_i^{(0)}, b_i^{(0)}) < E_i(\mathbf{0}, 0)$  is satisfied by a random initialization of  $\{\omega_i^{(0)}, b_i^{(0)}\}$  around  $\mathbf{0}$  under some mild conditions; see [36, Theorem 5.4]. In the following, we consider a generalization of Proposition 4.2 for the general  $F$ . We show that any nontrivial critical point has a lower energy than the flat energy region consisting of dead neurons.

THEOREM 4.3. *In the single neuron problem (4.4), any critical point  $\{\omega_i^*, b_i^*\} \in \mathbb{R}^{d+1}$  such that  $\sigma(\omega_i^* \cdot x + b_i^*) \not\equiv 0$  on  $\Omega$  satisfies  $E_i(\omega_i^*, b_i^*) < E_i(\mathbf{0}, 0)$ .*

*Proof.* Since  $\sigma(\omega_i^* \cdot x + b_i^*)$  is nontrivial on  $\Omega$ , the set

$$D = \{x \in \Omega : \omega_i^* \cdot x + b_i^* > 0\}$$

has nonzero measure. Note that  $\sigma(\omega_i^* \cdot x + b_i^*) = \omega_i^* \cdot x + b_i^*$  and  $\sigma'(\omega_i^* \cdot x + b_i^*) = 1$  on  $D$ . Since  $\nabla E_i(\omega_i^*, b_i^*) = \mathbf{0}$ , we obtain

$$(4.6) \quad \begin{aligned} \mathbf{0} = \nabla E_i(\omega_i^*) &= \int_{\Omega} (\mathcal{A}\sigma(\omega_i^* \cdot x + b_i^*) - F(x)) \sigma'(\omega_i^* \cdot x + b_i^*) \begin{bmatrix} x \\ 1 \end{bmatrix} dx \\ &= \int_D (\mathcal{A}(\omega_i^* \cdot x + b_i^*) - F(x)) \begin{bmatrix} x \\ 1 \end{bmatrix} dx, \end{aligned}$$

where the operator  $\mathcal{A}$  was given in (3.4) and the integrals are done entrywise. It follows that

$$\begin{aligned} E_i(\omega_i^*, b_i^*) &= \frac{1}{2} \int_D [\mathcal{A}(\omega_i^* \cdot x + b_i^*)] (\omega_i^* \cdot x + b_i^*) dx - \int_D F(x) (\omega_i^* \cdot x + b_i^*) dx \\ &= \begin{bmatrix} \omega_i^* \\ b_i^* \end{bmatrix} \cdot \int_D [\mathcal{A}(\omega_i^* \cdot x + b_i^*) - F(x)] \begin{bmatrix} x \\ 1 \end{bmatrix} dx - \frac{1}{2} \int_D [\mathcal{A}(\omega_i^* \cdot x + b_i^*)] (\omega_i^* \cdot x + b_i^*) dx \\ &\stackrel{(4.6)}{=} -\frac{1}{2} \int_D [\mathcal{A}(\omega_i^* \cdot x + b_i^*)] (\omega_i^* \cdot x + b_i^*) dx \\ &< 0 = E_i(\mathbf{0}, 0), \end{aligned}$$

which completes the proof.  $\square$

Thanks to [Theorem 4.3](#), we can ensure that choosing an initial guess  $\{\omega_i^{(0)}, b_i^{(0)}\}$  such that  $E_i(\omega_i^{(0)}, b_i^{(0)}) < E_i(\mathbf{0})$  makes the training algorithm to converge to a good local minimum that prevents the neuron to be dead. That is, the  $\{\omega_i, b_i\}$ -minimization problems of NPSC do not produce dead neurons.

Various optimization algorithms including first- and second-order methods can be used to solve (4.4). Among them, a good option is the Levenberg–Marquardt algorithm [20]; PDEs usually arise from physics, so that the dimension  $d+1$  of  $\{\omega_i, b_i\}$  is not very big in general. The major computational cost of each iteration of the Levenberg–Marquardt algorithm is to solve a linear system with  $d+1$  unknowns; it is not time-consuming when  $d+1$  is small. The Levenberg–Marquardt algorithm does not require explicit assembly of the Hessian, and it converges to a local minimum with the superlinear convergence rate [41], which is much faster than other first-order methods.

**4.4. Backtracking for learning rates.** We now discuss the use of a backtracking scheme to find a suitable value for the learning rate  $\tau_k$  in [Algorithm 4.1](#). It was recently shown in [24] that parallel subspace correction methods for convex optimization problems can be accelerated by adopting a backtracking scheme. Although, due to the nonconvexity and nonsmoothness of the loss function  $E$  of (2.3), we are not able to adopt the backtracking scheme proposed in [24] or the conventional backtracking schemes such as [7, 28] directly to [Algorithm 4.1](#), a simple but effective backtracking scheme for finding  $\tau_k$  presented in [Algorithm 4.3](#) can still be used. By allowing adaptive increase and decrease of  $\tau_k$  along the epochs, the convergence rate of NPSC is improved.

---

**Algorithm 4.3** Backtracking scheme to find  $\tau_k$  in [Algorithm 4.1](#)

---

```

Choose a minimum learning rate  $\tau_{\min} = 10^{-12}$ .
 $\tau_k \leftarrow 2\tau_{k-1}$ 
repeat
  for  $i = 1, \dots, n$  in parallel do
     $\hat{\omega}_i = (1 - \tau_k)\omega_i^{(k)} + \tau_k\omega_i^{(k+\frac{1}{2})}$ 
     $\hat{b}_i = (1 - \tau_k)b_i^{(k)} + \tau_k b_i^{(k+\frac{1}{2})}$ 
  end for
  if  $E(\{a^{(k+1)}, \hat{\omega}, \hat{b}\}) > E(\{a^{(k+1)}, \omega^{(k)}, b^{(k)}\})$  then
     $\tau_k \leftarrow \tau_k/2$ 
  end if
until  $E(\{a^{(k+1)}, \hat{\omega}, \hat{b}\}) \leq E(\{a^{(k+1)}, \omega^{(k)}, b^{(k)}\})$  or  $\tau_k < \tau_{\min}$ 

```

---

**5. Numerical experiments.** In this section, we present numerical results of NPSC applied to various function approximation problems and PDEs of the form (2.3). The following algorithms are compared with NPSC in our numerical experiments: gradient descent (GD), Adam [15], hybrid least-squares/gradient descent (LSGD) [9]. All the algorithms were implemented in ANSI C with OpenMPI compiled by Intel C++ Compiler. They were executed on a computer cluster equipped with multiple Intel Xeon SP-6148 CPUs (2.4GHz, 20C) and the operating system CentOS 7.4 64bit.

In all experiments, we use the He initialization [12] to initialize the parameters of (2.3). That is, we set  $a_i \sim N(0, 2/n)$ ,  $\omega_i \sim (N(0, 2/d))^d$ , and  $b_i \sim (N(0, 2/d))$  in (2.3). All the numerical results presented in this section are averaged over 10 random initializations. As shown in [Appendix B](#), the performances of conventional

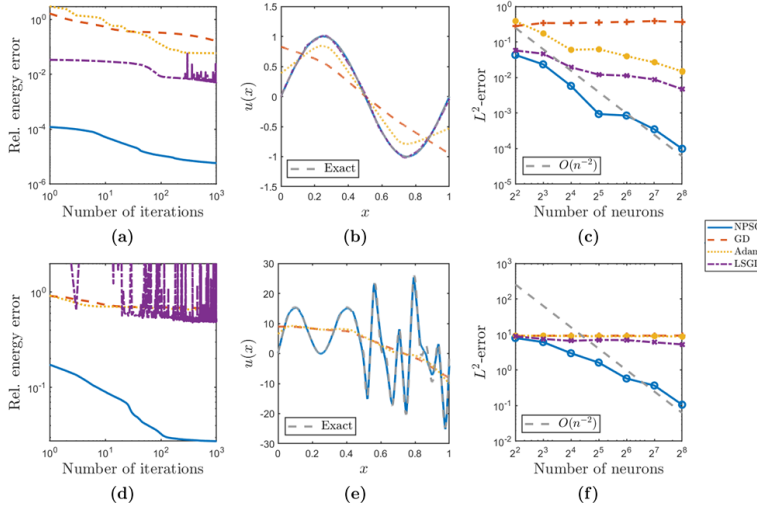


FIG. 3. Numerical results for the function approximation problems (a–c) (5.2) and (d–f) (5.3). (a, d) Decay of the relative energy error  $\frac{E(\theta^{(k)}) - E^*}{|E^*|}$  in various training algorithms ( $n = 2^5$ ). (b, e) Exact solution and its approximations ( $n = 2^5, 10^3$  epochs). (c, f)  $L^2$ -errors with respect to the number of neurons ( $10^3$  epochs). The dotted line represents the theoretical optimal approximation rate.

training algorithms can be improved by utilizing the backtracking scheme presented in Algorithm 4.3. Hence, for GD, Adam, and LSGD, we employ Algorithm 4.3 to find learning rates. In LSGD and NPSC,  $\alpha$ -minimization problems (4.3) are solved by the preconditioned conjugate gradient method with the preconditioner  $P$  in Theorem 3.2 and the stop criterion

$$(5.1) \quad \frac{\|Ka^{(k)} - \beta\|_{\ell^2}}{\|Ka^{(0)} - \beta\|_{\ell^2}} < 10^{-10}.$$

Finally,  $\{\omega_i, b_i\}$ -minimization problems (4.4) in NPSC are solved by the Levenberg–Marquardt algorithm [20] with the stop criterion

$$\frac{|E_i^{(n-1)} - E_i^{(n)}|}{|E_i^{(n)}|} < 10^{-10}.$$

MPI parallelization is applied to NPSC in a way that each  $\{\omega_i, b_i\}$ -minimization problem is assigned to a single processor and solved in parallel.

**5.1.  $L^2$ -function approximation problems.** If we set (2.4) in (2.3), then we obtain the  $L^2$ -function approximation problem, which is the most elementary instance of (2.3). That is, the solution of (2.3) in this case is the best  $L^2$ -approximation of  $f$  found in  $\Sigma_n$ . As our first example, we consider  $L^2$ -approximation (2.4) for a sine function; we set

$$(5.2) \quad \Omega = (0, 1) \subset \mathbb{R}, \quad f(x) = \sin 2\pi x$$

in (2.3). For numerical integration, we use the trapezoidal rule on 10,000 uniformly sampled points; see Appendix C. Figure 3(a) plots the relative energy errors  $\frac{E(\theta^{(k)}) - E^*}{|E^*|}$

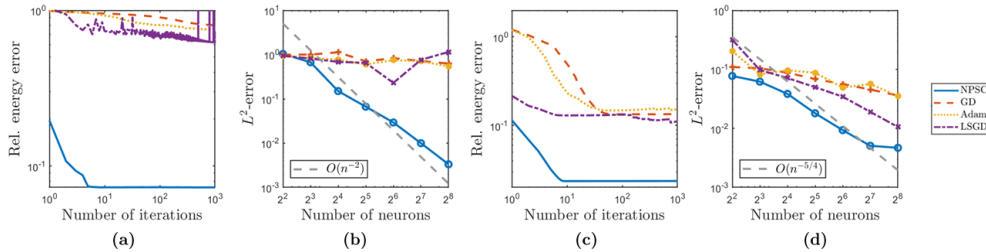


FIG. 4. Numerical results for the elliptic PDEs (a, b) (5.5) and (c, d) (5.6). (a, c) Decay of the relative energy error  $\frac{E(\theta^{(k)}) - E^*}{|E^*|}$  in various training algorithms ( $n = 2^5$ ). (b, d)  $L^2$ -errors with respect to the number of neurons ( $10^3$  epochs). The dotted line represents the theoretical optimal approximation rate.

obtained by NPSC, GD, Adam, and LSGD per epoch, where  $E^*$  is the loss corresponding to the exact solution. It is clear from the loss decay that NPSC outperforms all the other methods. The exact solution of (5.2) and its approximations obtained by  $10^3$  epochs of the training algorithms with  $2^5$  neurons are depicted in Figure 3(b). One can readily observe that the NPSC result is most accurate among the approximations. The  $L^2$ -errors between the exact solution and its approximations for various numbers of neurons are presented in Figure 3(c). Only the NPSC result seems to be comparable to  $O(n^{-2})$ , the theoretical optimal rate derived in [31].

We revisit (2.6) as the second example, a highly oscillatory instance of (2.4):

$$(5.3) \quad \Omega = (0, 1) \subset \mathbb{R}, \quad f(x) = \begin{cases} 10(\sin 2\pi x + \sin 6\pi x), & \text{if } 0 \leq x < \frac{1}{2}, \\ 10(\sin 8\pi x + \sin 18\pi x + \sin 26\pi x), & \text{if } \frac{1}{2} \leq x \leq 1, \end{cases}$$

in which a similar problem appeared in [6]. We note that it was demonstrated in [17] that training for complex functions like (5.3) is a much harder task than training for simple functions. Same as in (5.2), we use the trapezoidal rule on 10,000 uniformly sampled points for numerical integration. Figure 3(d–f) present numerical results for the problem (5.3). In Figure 3(d), NPSC shows stable decay of the loss while the losses of GD and Adam are stagnant along the epochs and that of LSGD blows up at the beginning epochs and varies very rapidly. In Figure 3(e), one can observe that the NPSC result captures both low- and high-frequency parts of the target function well, while the other ones capture the low-frequency part only [40]. Moreover, as shown in Figure 3(f), the  $L^2$ -error of the NPSC decreases when the number of neurons increases, while those of the other algorithms seem to stagnate. This highlights the robustness of NPSC for complex problems.

**5.2. Elliptic PDEs.** Next, we consider the case

$$(5.4) \quad V = H^1(\Omega), \quad a(u, v) = \int_{\Omega} (\nabla u \cdot \nabla v + uv) \, dx, \quad u, v \in V$$

in the problem (2.3), where  $H^1(\Omega)$  is the usual Sobolev space consisting of  $L^2(\Omega)$ -functions with square-integrable gradients. It is well-known that (2.3) becomes the Galerkin approximation of the weak formulation of the following elliptic PDE on

$n$	Problem (5.3)		Problem (5.5)	
	Prec.	Unprec.	Prec.	Unprec.
$2^4$	2	34	3	19
$2^5$	2	107	2	37
$2^6$	2	310	4	59
$2^7$	3	1018	4	103
$2^8$	3	3470	5	173

TABLE 1

Number of preconditioned and unpreconditioned conjugate gradient iterations to solve the  $a$ -minimization problems (3.1) corresponding to the  $L^2$ -function approximation problem (5.3) and the elliptic PDE (5.5), where  $n$  denotes the number of neurons.

$\Sigma_n$  [39]:

$$-\Delta u + u = f \quad \text{in } \Omega, \quad \frac{\partial u}{\partial n} = 0 \quad \text{on } \partial\Omega,$$

where  $\partial u/\partial n$  denotes the normal derivative of  $u$  to  $\partial\Omega$ . Hence, one can find a numerical approximation for the solution of the above PDE by solving (5.4). We set

$$(5.5) \quad \Omega = (0, 1) \subset \mathbb{R}, \quad f(x) = (1 + 9\pi^2) \cos 3\pi x + (1 + 121\pi^2) \cos 11\pi x$$

in (5.4). The exact solution is  $u(x) = \cos 3\pi x + \cos 11\pi x$ . We can observe in Figure 4(a) that NPSC achieves a superior level of accuracy such that the other algorithms do not reach even with a large number of epochs. As shown in Figure 4(b),  $L^2$ -errors of the NPSC results decrease as the number of neuron increases, and their decreasing rates are comparable to the theoretical optimal rates in [31].

Finally, we consider the following two-dimensional example for (5.4):

$$(5.6) \quad \Omega = (0, 1)^2 \subset \mathbb{R}^2, \quad f(x_1, x_2) = (1 + 2\pi^2) \cos \pi x_1 \cos \pi x_2,$$

whose exact solution is  $u(x_1, x_2) = \cos \pi x_1 \cos \pi x_2$ . Since the preconditioner in Theorem 3.2 is applicable for one-dimension only, in this example,  $a$ -minimization problems are solved by  $n$  iterations of the unpreconditioned conjugate gradient method. We use the quasi-Monte Carlo method [5] with 10,000 sampling points for numerical integration; see Appendix C for details. It is verified by the numerical results for (5.6) presented in Figure 4(c, d) that NPSC outperforms the other methods and provides reasonable  $L^2$ -errors in high-dimensional problems as well.

*Remark 5.1.* When we train a neural network (2.2) for solving the PDE (5.4) with a gradient-based method, we have to evaluate the second-order derivative of  $\sigma(x)$ , which is the Dirac delta function. In our experiments, we simply ignore Dirac delta terms in numerical integration. This motivates us to consider high-order activation functions like  $\text{ReLU}^k$  [29] as a future work.

**5.3. Effect of preconditioning.** We present some numerical results to highlight the computational efficiency of the preconditioner  $P$ . The  $a$ -minimization problems (4.3) appearing in training of neural networks that solve the  $L^2$ -function approximation problem (5.3) and the elliptic boundary value problem (5.5) are considered. We set the parameters  $\omega$  and  $b$  in the nonlinear layer as follows:

$$\omega_i = 1, \quad b_i = -\frac{i}{n+1}, \quad 1 \leq i \leq n.$$



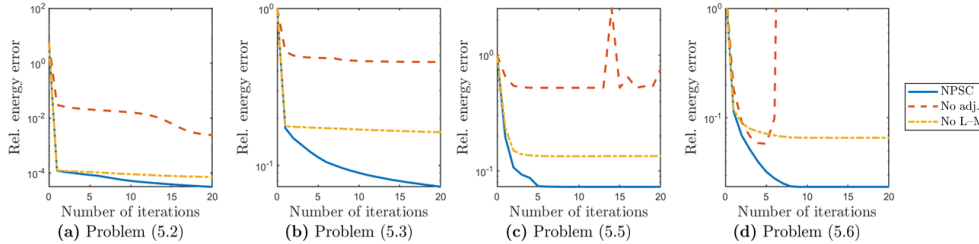


FIG. 5. Ablation studies for NPSC on the relative energy error  $\frac{E(\theta^{(k)}) - E^*}{|E^*|}$ . “No adj.” and “No L-M” denote NPSC without the adjustment step and the Levenberg–Marquardt algorithm, respectively.

We compare the numerical performances of the preconditioned and unpreconditioned conjugate gradient methods solving (4.3). The initial guess  $a^{(0)}$  is given by the zero vector. Table 1 presents the number of iterations of the preconditioned and unpreconditioned conjugate gradient methods to meet the stop condition (5.1) with respect to various numbers of neurons  $n$ . While the number of unpreconditioned iterations increases rapidly as  $n$  increases, the number of preconditioned iterations is uniformly bounded with respect to  $n$ . This supports our theoretical result presented in Theorem 3.2, which claims that the condition number of the preconditioned operator  $PK$  is  $O(1)$ . Since the computational cost of  $P$  is cheap, we can conclude that the preconditioner  $P$  is numerically efficient.

**5.4. Ablation studies.** Key components of the proposed NPSC are the adjustment step for parameters (Algorithm 4.2), the optimal preconditioner for the linear layer (Theorem 3.2), the Levenberg–Marquardt algorithm for  $\{\omega_i, b_i\}$ -minimization problems, and the backtracking scheme for learning rates (Algorithm 4.3). In order to validate the effects of these components, we conduct ablation studies for the adjustment step and the Levenberg–Marquardt algorithm; relevant results for the backtracking scheme can be found in Appendix B.

Figure 5 depicts numerical comparisons among three algorithms: NPSC, NPSC without Algorithm 4.2, and NPSC without the Levenberg–Marquardt algorithm. In the last algorithm, each  $\{\omega_i, b_i\}$ -minimization problem is solved approximately by 20 iterations of GD. Since the variants of NPSC achieve slower convergence rates than NPSC in all the examples, one can conclude that both Algorithm 4.2 and the Levenberg–Marquardt algorithm contribute to the fast convergence of NPSC. We also note that Algorithm 4.2 helps NPSC to avoid unstable convergence behaviors like Figure 5(c, d).

**6. Conclusion.** In this paper, we proposed NPSC for the finite neuron method with ReLU neural networks. Separately designing efficient solvers for the linear layer and each neuron and training them alternately, NPSC yields accurate results for function approximation problems and PDEs.

This paper leaves us several interesting and important topics for future research. Although NPSC adopts the well-established framework of subspace correction methods, its rigorous convergence analysis is still open due to the nonconvexity of the model. To solve high-order PDEs, we should generalize NPSC so that it can be applied to different kind of activation functions. In addition, we should consider optimal preconditioners for optimizing linear layer in high dimensions. Generalization

of NPSC to many layers is not clear yet, and we consider this topic as a future work.

Reducing the gap between the theoretical approximation properties and training results is a challenging issue even for simple neural networks. To the best of our knowledge, NPSC is the first result that deals with the ill-conditioning of layers and successfully reduces the gap. We believe that this paper can play a role of a good preliminary work for efficient and accurate training of general network architectures.

### Appendix A. Implementation details for the optimal preconditioner.

In this appendix, we discuss the computational aspects of the proposed preconditioner. Although the preconditioner  $P$  defined in (3.15) seems a bit complicated at the first glance, its computation requires only a cheap cost. We provide a detailed explanation of how to apply the preconditioner  $P$  efficiently.

Three nontrivial parts in the preconditioner  $P$  are the inverses of the matrices  $B_1$ ,  $\bar{K}_\phi$ , and  $R\bar{P}^{-1}R^T$ . First, we consider how to compute  $B_1^{-1}\alpha$  when a vector  $\alpha \in \mathbb{R}^{n_\Omega+2}$  is given. We solve a linear system  $B_1\beta = \alpha$  in order to obtain  $B_1^{-1}\alpha$ . Thanks to the sparsity pattern of  $B_1$ , this linear system can be solved directly by the following  $O(n)$  elementary arithmetic operations:

$$\beta_i = \begin{cases} \frac{1}{(B_1)_{ii}} \left( \alpha_i - \frac{(B_1)_{i,n_\Omega+1}}{(B_1)_{n_\Omega+1,n_\Omega+1}} \alpha_{n_\Omega+1} - \frac{(B_1)_{i,n_\Omega+2}}{(B_1)_{n_\Omega+2,n_\Omega+2}} \alpha_{n_\Omega+2} \right), & \text{if } 1 \leq i \leq n_\Omega, \\ \frac{\alpha_i}{(B_1)_{ii}}, & \text{otherwise.} \end{cases}$$

Secondly, we consider how to compute  $\bar{K}_\phi^{-1}\alpha$  when a vector  $\alpha \in \mathbb{R}^{n_\Omega+2}$  is given. In most applications, the bilinear form  $a(\cdot, \cdot)$  is defined in terms of differential operators as in (5.4). This implies that the matrix  $\bar{K}_\phi$  is tridiagonal, so that  $\bar{K}_\phi^{-1}\alpha$  can be obtained by the Thomas algorithm (see, e.g., [13, Section 9.6]), which requires only  $O(n)$  elementary arithmetic operations.

Finally, we discuss how to compute  $(R\bar{P}^{-1}R^T)^{-1}\alpha$  for  $\alpha \in \mathbb{R}^n$ . Similarly, one can compute it by solving a linear system

$$R\bar{P}^{-1}R^T\beta = \alpha.$$

By the definition (3.7) of  $R$ , we have

$$\bar{P}^{-1}R^T\beta = \begin{bmatrix} \alpha_{1:n_\Omega} \\ \gamma \end{bmatrix}$$

for some  $\gamma \in \mathbb{R}^2$ , where  $1:n_\Omega$  means ‘‘from the first to  $n_\Omega$ th entries.’’ One can readily deduce that  $\gamma$  is determined by the following two relations:

$$(A.1a) \quad \tilde{R}\gamma = \alpha_{(n_\Omega+1):n},$$

$$(A.1b) \quad \left( \bar{P} \begin{bmatrix} \alpha_{1:n_\Omega} \\ \gamma \end{bmatrix} \right)_{(n_\Omega+1):(n_\Omega+2)} \in \text{ran } \tilde{R}^T.$$

Now,  $\beta$  is then given by

$$\begin{aligned} \beta_{1:n_\Omega} &= \left( \bar{P} \begin{bmatrix} \alpha_{1:n_\Omega} \\ \gamma \end{bmatrix} \right)_{1:n_\Omega}, \\ \tilde{R}^T\beta_{(n_\Omega+1):n} &= \left( \bar{P} \begin{bmatrix} \alpha_{1:n_\Omega} \\ \gamma \end{bmatrix} \right)_{(n_\Omega+1):(n_\Omega+2)}. \end{aligned}$$

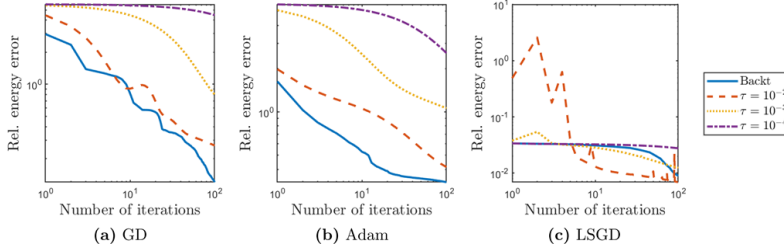


FIG. 6. Decay of the relative energy error  $\frac{E(\theta^{(k)}) - E^*}{|E^*|}$  in various training algorithms for solving (5.2). “Backt” denotes the backtracking scheme presented in Algorithm 4.3, and  $\tau$  denotes the fixed learning rate.

Since  $\tilde{R} \in \mathbb{R}^{(n-n_\Omega) \times 2}$ , (A.1a) and (A.1b) are written as  $n - n_\Omega$  and  $2 - (n - n_\Omega)$  linear equations, respectively. That is,  $\gamma$  can be determined by solving the system (A.1) of two linear equations.

We now deal with how to solve the linear system (A.1) algebraically in detail. We write  $\gamma = [\gamma_1, \gamma_2]^T \in \mathbb{R}^2$ . By (3.3b), the number of interior nodal points  $n_\Omega$  is either  $n - 2$ ,  $n - 1$ , or  $n$ . First, we consider the case  $n_\Omega = n - 2$ . In this case, (A.1b) obviously holds and (A.1a) reads as

$$(A.2a) \quad \psi_{n_\Omega+1}(1)\gamma_1 + \psi_{n_\Omega+1}(0)\gamma_2 = \alpha_{n_\Omega+1},$$

$$(A.2b) \quad \psi_{n_\Omega+2}(1)\gamma_1 + \psi_{n_\Omega+2}(0)\gamma_2 = \alpha_{n_\Omega+2}.$$

Hence, one can find  $\gamma$  by solving (A.2) directly.

Next, we assume that  $n_\Omega = n - 1$ . Then (A.1a) and (A.1b) read as (A.2a) and (A.3)

$$\bar{P}_{(n_\Omega+1):(n_\Omega+2),1:n_\Omega} \alpha_{1:n_\Omega} + \bar{P}_{(n_\Omega+1):(n_\Omega+2),(n_\Omega+1):(n_\Omega+2)} \gamma \in \text{span} \left\{ \begin{bmatrix} \psi_{n_\Omega+1}(1) \\ \psi_{n_\Omega+1}(0) \end{bmatrix} \right\},$$

respectively. Since (A.3) is equivalent to

$$(A.4) \quad (\bar{P}_{n_\Omega+1,1:n_\Omega} \alpha_{1:n_\Omega} + \bar{P}_{n_\Omega+1,(n_\Omega+1):(n_\Omega+2)} \gamma) \psi_{n_\Omega+1}(0) - (\bar{P}_{n_\Omega+2,1:n_\Omega} \alpha_{1:n_\Omega} + \bar{P}_{n_\Omega+2,(n_\Omega+1):(n_\Omega+2)} \gamma) \psi_{n_\Omega+1}(1) = 0,$$

$\gamma$  can be obtained by solving the linear system consisting of (A.2a) and (A.4).

Finally, we consider the case  $n_\Omega = n$ . In this case, (A.1a) is void and (A.1b) reads as

$$\bar{P}_{(n_\Omega+1):(n_\Omega+2),1:n_\Omega} \alpha_{1:n_\Omega} + \bar{P}_{(n_\Omega+1):(n_\Omega+2),(n_\Omega+1):(n_\Omega+2)} \gamma = 0.$$

Therefore,  $\gamma$  is found by solving the above linear system.

In summary, the optimal preconditioner requires only  $O(n)$  elementary arithmetic operations.

**Appendix B. Effect of backtracking for conventional training algorithms.** In this appendix, we present numerical results that show that the backtracking scheme presented in Algorithm 4.3 is useful not only for the proposed NPSC but also for conventional training algorithms such as GD, Adam [15], and LSGD [9].

Figure 6 plots the relative energy error  $\frac{E(\theta^{(k)}) - E^*}{|E^*|}$  of GD, Adam, and LSGD for solving the problem (5.2), averaged over 10 random initializations, where  $k$  denotes

the number of epochs and  $E^*$  is the energy corresponding to the exact solution of the problem. The number of neurons used is  $2^5$ ; while we can observe similar results for the other numbers of neurons, we only provide the result of  $2^5$  neurons for brevity. We observe that the algorithms equipped with the backtracking scheme outperform those with constant learning rates  $\tau = 10^{-2}$ ,  $10^{-3}$ , and  $10^{-4}$  in the sense of the convergence rate. That is, [Algorithm 4.3](#) seems to successfully find a good learning rate at each iteration of conventional training algorithms as well. Hence, in [section 5](#), we employ [Algorithm 4.3](#) to find learning rates of GD, Adam, and LSGD.

**Appendix C. Numerical integration.** This appendix is devoted to numerical integration schemes for computing the integral in our model problem [\(2.3\)](#). If  $d = 1$ , i.e., if the domain  $\Omega = (0, 1) \subset \mathbb{R}$ , then we approximate the integral of a function  $g(x)$  defined on  $\Omega$  by the following simple trapezoidal rule:

$$(C.1) \quad \int_{\Omega} g(x) dx \approx \sum_{j=1}^{N-1} \frac{g(x_j) + g(x_{j+1})}{2} (x_{j+1} - x_j),$$

where  $0 = x_1 < x_2 < \dots < x_N = 1$  are  $N$  uniform sampling points between 0 and 1, i.e.,  $x_j = \frac{j-1}{N-1}$ ,  $1 \leq j \leq N$ . Approximation properties of the trapezoidal rule [\(C.1\)](#) can be found in standard textbooks on numerical analysis; see, e.g., [\[4\]](#).

When  $d \geq 2$ , we adopt the quasi-Monte Carlo method [\[5\]](#) based on Halton sequences [\[16\]](#), which is known to overcome the curse of dimensionality in the sense that approximation error bounds independent of the dimension  $d$  are available. In the quasi-Monte Carlo method, the integral of a function  $g(x)$  defined on  $\Omega$  is approximated by the average of the function evaluated at  $N$  sampling points:

$$(C.2) \quad \int_{\Omega} g(x) dx \approx \frac{1}{N} \sum_{j=1}^N g(x_j),$$

where  $\{x_j\}_{j=1}^N$  is a low-discrepancy sequence in  $\Omega$  defined in terms of Halton sequences. For the sake of description, we assume that  $\Omega = (0, 1)^d \in \mathbb{R}^d$ . Then the  $k$ th coordinate of  $x_j$  ( $1 \leq j \leq N$ ,  $1 \leq k \leq d$ ) is the number  $j$  written in  $p_k$ -ary representation, inverted, and written after the decimal point, where  $p_k$  is the  $k$ th smallest prime number. For example, if  $d = 3$ , then the first four points of  $\{x_j\}_{j=1}^N$  is given by

$$x_1 = \left( \frac{1}{2}, \frac{1}{3}, \frac{1}{5} \right), \quad x_2 = \left( \frac{1}{2^2}, \frac{2}{3}, \frac{2}{5} \right), \quad x_3 = \left( \frac{3}{2^2}, \frac{1}{3^2}, \frac{3}{5} \right), \quad x_4 = \left( \frac{1}{2^3}, \frac{4}{3^2}, \frac{4}{5} \right).$$

Approximation properties of [\(C.2\)](#) can be found in [\[5\]](#).

#### REFERENCES

- [1] M. AINSWORTH AND Y. SHIN, *Plateau phenomenon in gradient descent training of ReLU networks: Explanation, quantification, and avoidance*, SIAM J. Sci. Comput., 43 (2021), pp. A3438–A3468.
- [2] M. AINSWORTH AND Y. SHIN, *Active Neuron Least Squares: A training method for multivariate rectified neural networks*, SIAM J. Sci. Comput., 44 (2022), pp. A2253–A2275.
- [3] L. BADEA AND R. KRAUSE, *One-and two-level Schwarz methods for variational inequalities of the second kind and their application to frictional contact*, Numer. Math., 120 (2012), pp. 573–599.
- [4] R. L. BURDEN, J. D. FAIRES, AND A. M. BURDEN, *Numerical Analysis*, Cengage Learning, Boston, MA, 2015.

- [5] R. E. CAFLISCH, *Monte Carlo and quasi-Monte Carlo methods*, Acta Numer., 7 (1998), pp. 1–49.
- [6] W. CAI, X. LI, AND L. LIU, *A phase shift deep neural network for high frequency approximation and wave problems*, SIAM J. Sci. Comput., 42 (2020), pp. A3285–A3312.
- [7] L. CALATRONI AND A. CHAMBOLLE, *Backtracking strategies for accelerated descent methods with smooth composite objectives*, SIAM J. Optim., 29 (2019), pp. 1772–1798.
- [8] G. CYBENKO, *Approximation by superpositions of a sigmoidal function*, Math. Control Signals Syst., 2 (1989), pp. 303–314.
- [9] E. C. CYR, M. A. GULIAN, R. G. PATEL, M. PEREGO, AND N. A. TRASK, *Robust training and initialization of deep neural networks: An adaptive basis viewpoint*, in Proceedings of The First Mathematical and Scientific Machine Learning Conference, vol. 107 of Proceedings of Machine Learning Research, PMLR, 2020, pp. 512–536.
- [10] W. E AND B. YU, *The deep Ritz method: a deep learning-based numerical algorithm for solving variational problems*, Commun. Math. Stat., 6 (2018), pp. 1–12.
- [11] J. HE, L. LI, J. XU, AND C. ZHENG, *ReLU deep neural networks and linear finite elements*, J. Comput. Math., 38 (2020), pp. 502–527.
- [12] K. HE, X. ZHANG, S. REN, AND J. SUN, *Delving deep into rectifiers: Surpassing human-level performance on ImageNet classification*, in Proceedings of the IEEE International Conference on Computer Vision, 2015, pp. 1026–1034.
- [13] N. J. HIGHAM, *Accuracy and Stability of Numerical Algorithms*, SIAM, Philadelphia, PA, second ed., 2002.
- [14] Q. HONG, J. W. SIEGEL, Q. TAN, AND J. XU, *On the activation function dependence of the spectral bias of neural networks*, arXiv preprint arXiv:2208.04924, (2022).
- [15] D. P. KINGMA AND J. BA, *Adam: A method for stochastic optimization*, in 3rd International Conference on Learning Representations, ICLR 2015, San Diego, CA, USA, May 7-9, 2015, Conference Track Proceedings, 2015.
- [16] L. KOCIS AND W. J. WHITEN, *Computational investigations of low-discrepancy sequences*, ACM Trans. Math. Software, 23 (1997), pp. 266–294.
- [17] A. KRISHNAPRIYAN, A. GHOLAMI, S. ZHE, R. KIRBY, AND M. W. MAHONEY, *Characterizing possible failure modes in physics-informed neural networks*, in Advances in Neural Information Processing Systems, vol. 34, Curran Associates, Inc., 2021, pp. 26548–26560.
- [18] C.-O. LEE AND J. PARK, *Fast nonoverlapping block Jacobi method for the dual Rudin–Osher–Fatemi model*, SIAM J. Imaging Sci., 12 (2019), pp. 2009–2034.
- [19] L. LU, Y. SHIN, Y. SU, AND G. E. KARNIADAKIS, *Dying ReLU and initialization: Theory and numerical examples*, Commun. Comput. Phys., 28 (2020), pp. 1671–1706.
- [20] D. W. MARQUARDT, *An algorithm for least-squares estimation of nonlinear parameters*, J. Soc. Ind. Appl. Math., 11 (1963), pp. 431–441.
- [21] J. NOCEDAL AND S. J. WRIGHT, *Numerical Optimization*, Springer, New York, second ed., 2006.
- [22] H. PARK, S.-I. AMARI, AND K. FUKUMIZU, *Adaptive natural gradient learning algorithms for various stochastic models*, Neural Netw., 13 (2000), pp. 755–764.
- [23] J. PARK, *Additive Schwarz methods for convex optimization as gradient methods*, SIAM J. Numer. Anal., 58 (2020), pp. 1495–1530.
- [24] J. PARK, *Additive Schwarz methods for convex optimization with backtracking*, Comput. Math. Appl., 113 (2022), pp. 332–344.
- [25] A. PINKUS, *Approximation theory of the MLP model in neural networks*, Acta Numer., 8 (1999), pp. 143–195.
- [26] M. RAISSI, P. PERDIKARIS, AND G. E. KARNIADAKIS, *Physics-informed neural networks: A deep learning framework for solving forward and inverse problems involving nonlinear partial differential equations*, J. Comput. Phys., 378 (2019), pp. 686–707.
- [27] Y. SAAD, *Iterative Methods for Sparse Linear Systems*, SIAM, Philadelphia, 2003.
- [28] K. SCHEINBERG, D. GOLDFARB, AND X. BAI, *Fast first-order methods for composite convex optimization with backtracking*, Found. Comput. Math., 14 (2014), pp. 389–417.
- [29] J. W. SIEGEL AND J. XU, *High-order approximation rates for shallow neural networks with cosine and ReLU<sup>k</sup> activation functions*, Appl. Comput. Harmon. Anal., 58 (2022), pp. 1–26.
- [30] J. W. SIEGEL AND J. XU, *Optimal convergence rates for the orthogonal greedy algorithm*, IEEE Trans. Inform. Theory, 68 (2022), pp. 3354–3361.
- [31] J. W. SIEGEL AND J. XU, *Sharp bounds on the approximation rates, metric entropy, and n-widths of shallow neural networks*, Found. Comput. Math., (2022), <https://doi.org/10.1007/s10208-022-09595-3>.
- [32] M. SOLTANOLKOTABI, *Learning ReLUs via gradient descent*, in Advances in Neural Information

- Processing Systems, vol. 30, 2017.
- [33] X.-C. TAI AND J. XU, *Global and uniform convergence of subspace correction methods for some convex optimization problems*, Math. Comp., 71 (2002), pp. 105–124.
  - [34] Y. TIAN, *An analytical formula of population gradient for two-layered ReLU network and its applications in convergence and critical point analysis*, in Proceedings of the 34th International Conference on Machine Learning, vol. 70, PMLR, 2017, pp. 3404–3413.
  - [35] A. TOSELLI AND O. WIDLUND, *Domain Decomposition Methods—Algorithms and Theory*, Springer, Berlin, 2005.
  - [36] G. VARDI, G. YEHUDAI, AND O. SHAMIR, *Learning a single neuron with bias using gradient descent*, in Advances in Neural Information Processing Systems, vol. 34, 2021.
  - [37] S. J. WRIGHT, *Coordinate descent algorithms*, Math. Program., 151 (2015), pp. 3–34.
  - [38] J. XU, *Iterative methods by space decomposition and subspace correction*, SIAM Rev., 34 (1992), pp. 581–613.
  - [39] J. XU, *Finite neuron method and convergence analysis*, Commun. Comput. Phys., 28 (2020), pp. 1707–1745.
  - [40] Z.-Q. J. XU, Y. ZHANG, T. LUO, Y. XIAO, AND Z. MA, *Frequency principle: Fourier analysis sheds light on deep neural networks*, Commun. Comput. Phys., 28 (2020), pp. 1746–1767.
  - [41] N. YAMASHITA AND M. FUKUSHIMA, *On the rate of convergence of the Levenberg-Marquardt method*, in Topics in Numerical Analysis, vol. 15 of Comput. Suppl., Springer, Vienna, 2001, pp. 239–249.
  - [42] G. YEHUDAI AND S. OHAD, *Learning a single neuron with gradient methods*, in Proceedings of Thirty Third Conference on Learning Theory, vol. 125 of Proceedings of Machine Learning Research, PMLR, 2020, pp. 3756–3786.
  - [43] J. ZENG, T. T.-K. LAU, S. LIN, AND Y. YAO, *Global convergence of block coordinate descent in deep learning*, in Proceedings of the 36th International Conference on Machine Learning, vol. 97, PMLR, 2019, pp. 7313–7323.
  - [44] Z. ZHANG AND M. BRAND, *Convergent block coordinate descent for training tikhonov regularized deep neural networks*, in Advances in Neural Information Processing Systems, vol. 30, Curran Associates, Inc., 2017.